

## PYROLYSIS KINETICS OF OIL SHALE FROM NORTHERN SONGLIAO BASIN IN CHINA

XUE HUA-QING<sup>(a, b)\*</sup>, LI SHU-YUAN<sup>(b)</sup>,  
WANG HONG-YAN<sup>(a)</sup>, ZHENG DE-WEN<sup>(a)</sup>,  
FANG CHAO-HE<sup>(a)</sup>

<sup>(a)</sup> Petrochina research institute of Petroleum Exploration & Development  
Langfang branch, Langfang of Hebei 065007, China

<sup>(b)</sup> State Key Laboratory of Heavy Oil Processing in China University of Petroleum  
Beijing 102249, China

*Pyrolysis experiments on northern Songliao basin oil shale were carried out by Rock-Eval analyzer at five different heating rates of 10, 15, 20, 25 and 30 °C/min. Pyrolysis characteristics of oil shale were investigated at different heating rates. Kinetic parameters of oil shale pyrolysis were determined by using Friedman procedure and global first-order kinetics. From Friedman procedure, it is concluded that most reactions occur with the activation energy of 165–545 kJ/mol. The linear relationship between activation energy and logarithm of frequency factor was obtained. The values of activation energy and frequency factor, deduced from the first-order equation case, are used to predict pyrolysis time. It is found that pyrolysis time is correlating with pyrolysis temperature.*

### Introduction

Oil shales, used directly as fuels and processed to produce shale oil and other chemicals and materials, are widely distributed throughout the world with known deposits in every continent. China is one of the many countries that have large oil shale deposits, which are estimated at  $6 \times 10^{13}$  tonnes and mainly located in the Songliao Basin Northeast China and the Junggar basin Northwest China [1]. Though investigations on the Junggar basin are preliminary, Prof. A. Carroll assumes that oil shale resources in the Northwest China are enormous, maybe even richer than in the Green River, Colorado, USA [2]. China Natural Petroleum Corporation is establishing the first oil shale pilot plant in the northern Songliao basin. The projected annual output is  $1.0 \times 10^5$  tonnes of shale oil refinery [3].

---

\* Corresponding author: e-mail [hqxue@petrochina.com.cn](mailto:hqxue@petrochina.com.cn)

Generally speaking, thermal decomposition of oil shale is the only recommended way to obtain liquid oil from the insoluble organic matter (kerogen). Kerogen is a complex substance consisting of large molecules consisting of carbon and hydrogen with nitrogen, sulfur and oxygen. The structure of kerogen depends on the occurrence of deposits, and is for the Green River basin approximately  $C_{200}H_{300}O_{11}N_5S$  with the average molecule weight over 3000 [4]. So, the mechanism and kinetics of kerogen decomposition can vary in a wide range.

The Rock-Eval apparatus (RE) has been routinely used in organic geochemistry for examining oil shale potential and maturity of different rock samples [5-10]. It is also used to study kinetics of thermal decomposition of kerogen at pyrolysis. For example, Johannes and Kruusement *et al.* [11] evaluated oil potential and pyrolysis kinetics of two Estonian shales by RE analysis. The first-order kinetics model was proposed to estimate the values of apparent activation energy ( $E$ ) and frequency factor ( $A$ ). Lewan, Hill and Ruble [12] used both RE and hydrous pyrolysis to study pyrolysis of oil shales from different areas of USA. The duration of oil generation as determined by kinetics derived from RE and hydrous pyrolysis was compared.

Although there were many RE analysis made for oil shale, the kinetic model was almost the first-order reaction. The duration of shale oil extraction has not been completely researched and is limited to extrapolation for various thermal decomposition temperatures. The purpose of the present work was to study pyrolysis characteristics and kinetic parameters of oil shale from northern Songliao basin, China. The study is based on non-isothermal pyrolysis experiments using Rock-Eval technique. In addition, mathematical equation for pyrolysis time is predicted for isothermal conditions using the kinetic constants found from experiments under nonisothermal conditions.

## Experimental

### Oil shale

The oil shale sample from northern Songliao basin of China was used in Rock-Eval experiments. The basic data characterizing oil shale are as follows (wt.%):

- Fischer assay: shale oil 13.06, coke 63.41, water 12.58, gas + losses 10.95;
- Proximate analysis: ash 34.39, volatiles 41.23,  $CO_2$  9.87;
- Elemental analysis: C 35.51, H 2.12, O 11.37, N 0.60, S 0.27.

Before the Rock-Eval experiments the oil shale sample was ground (< 200 meshes) to eliminate the effects of heat transfer and mass transfer on kinetic parameters. The sample was dried at constant temperature of 80 °C for about 3 hours to eliminate moisture.

### Rock-Eval analysis

Pyrolysis experiments on oil shale were carried out using RE apparatus. This technique uses temperature-programmed heating of a small amount of sample in the inert atmosphere of nitrogen (Fig. 1). The method enables to estimate petroleum potential of rock samples by pyrolysis according to a programmed-temperature pattern. Temperature programs are defined in order to distinguish, by a flame ionization detector (FID), thermo-vaporized free hydrocarbons and/or fragments from thermolabile compounds at 300 °C (peak S1), and potential hydrocarbons (kerogen) that can be released during thermal cracking of organic matter in the range of 300–600 °C (peak S2). In this work, evaluation of thermolabile compounds (S1) was not investigated and weight loss curves were obtained.

About 15 mg of oil shale was put into a sample crucible. Flow of nitrogen gas (around 50 ml/min) was fed into the system from a point below the sample. Pyrolysis temperature was measured by the first thermocouple (TC1) positioned just below the sample crucible. The second thermocouple (TC2) was used to ensure continuity of temperature control when the crucible was removed from the pyrolysis oven at the end of the analysis. Weight loss curves were obtained at five different constant heating rates of 10, 15, 20, 25 and 30 °C/min between 250–550 °C as shown in Fig. 2.

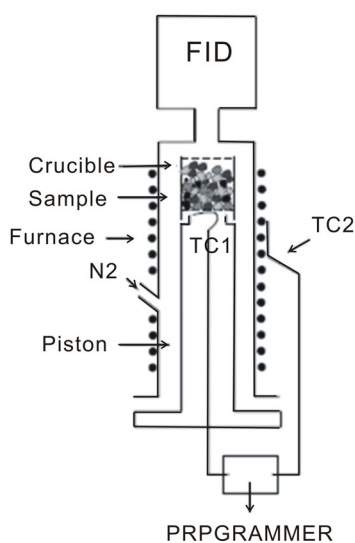


*Fig. 1.* Schematic diagram of ROCK-EVAL analyzer. Furnace open: temperature controlled by TC2; Furnace closed: temperature controlled by TC1; FID: flame ionization detector.

## Mathematical models

### Regression function

The equation used to determinate pyrolysis rate of oil shale is as follows [13]:

$$\begin{aligned} \frac{dx}{dt}(T) = & \frac{6}{h_j^2} \left[ \frac{1}{h_j} (T_{j+1} - T)^2 - (T_{j+1} - T) \right] x_j + \frac{6}{h_j^2} \left[ \frac{1}{h_j} (T - T_j) - \frac{1}{h_j} (T - T_j)^2 \right] x_{j+1} \\ & + \frac{1}{h_j} \left[ \frac{3}{h_j} (T_{j+1} - T)^2 - 2(T_{j+1} - T) \right] m_j - \frac{1}{h_j} \left[ 2(T - T_j) - \frac{3}{h_j} (T - T_j)^2 \right] m_{j+1} \end{aligned} \quad (1)$$

- $j$  point numbers  
 $h$  temperature interval  
 $m$  pyrolysis reaction rate  
 $x$  conversion  
 $k$  reaction rate constant,  $\text{min}^{-1}$   
 $n$  overall reaction order  
 $T$  temperature, K  
 $A$  frequency factor,  $\text{s}^{-1}$   
 $E$  activation energy,  $\text{J mol}^{-1}$   
 $R$  absolute gas constant ( $8.314 \text{ J mol}^{-1} \text{ K}^{-1}$ )  
 $t$  time, s

$m = dx/dt$  is the pyrolysis reaction rate,  $h = T_{j+1} - T_j$  is the temperature interval.

When solving equation, the boundary condition is as follows:

$$\left. \frac{d^2x}{dT^2} \right|_{x \rightarrow 0} = \left. \frac{d^2x}{dT^2} \right|_{x \rightarrow 1} = 0. \quad (2)$$

### Friedman procedure

According to the reaction theory, kinetic equation for decomposition of a solid is usually written:

$$\frac{dx}{dt} = k(1-x)^n. \quad (3)$$

In Eq. (3), according to Arrhenius equation, the expression of reaction rate constant  $k$  is as follows:

$$k = Ae^{-\frac{E}{RT}}. \quad (4)$$

When it is a first-order reaction, Eq. (4) can be substituted by Eq. (3) to give Eq. (5)

$$\frac{dx}{dt} = Ae^{-\frac{E}{RT}}(1-x). \quad (5)$$

The logarithm of Eq. (5) will yield following equation:

$$\ln \frac{dx}{dt} = \ln[A(1-x)] - \frac{E}{RT}. \quad (6)$$

For different heating rates, the temperatures required to reach the same conversion  $x$  and instantaneous reaction rate  $dx/dt$  differ for the same sample. A series of different values of fractional conversion  $x(x_1, x_2, x_3 \dots)$  are chosen as the constant. According to Eq. (6), the linear regression of  $dx/dt$  vs.  $1/T$  will determine the activation energy  $E$  and frequency factor  $A$  for each  $x$ .

### Global first-order reaction

In Eq. (5), at constant heating rate  $\beta = dT/dt$ , the following equation will be obtained:

$$\frac{dx}{dT} = \frac{A}{\beta} e^{-\frac{E}{RT}}(1-x), \quad (7)$$

where  $\beta$  is heating rate,  $K \text{ min}^{-1}$ .

The approximate integration of Eq. (7) will give Eq. (8):

$$\ln \left[ \frac{-\ln(1-x)(E+2RT)}{T^2} \right] = \ln \frac{AR}{\beta} - \frac{E}{RT}. \quad (8)$$

By using linear regression of  $\ln[-\ln(1-x)(E+2RT)/T^2]$  versus  $1/T$  in Eq. (8), the activation energy  $E$  and frequency factor  $A$  can be calculated by slope and intercept from regression, respectively. During the regression, the initial value of  $E$  has to be given in advance. When the calculated  $E$  equals the given  $E$ , the regression will be stopped.

### Pyrolysis time

By using the obtained kinetic parameters and conversion, the duration of oil shale pyrolysis at a constant temperature can be determined. It is a quite important information for the oil shale retorting process. In Eq. (5), if temperature  $T$  is regarded as constant, we can obtain the equation for pyrolysis time as follows:

$$t = -\frac{1}{A} e^{\frac{E}{RT}} \ln(1-x). \quad (9)$$

## Results and discussion

### Experimental data

Figure 2 shows the conversion of oil shale as a function of temperature at various heating rates obtained at the Rock-Eval analysis. It is seen from the figure that the changes of the trend curves at different heating rates are roughly the same. As the temperature increases, the conversion of oil shale also increases. It is due to the fact that oil shale pyrolysis process is continuous and irreversible.

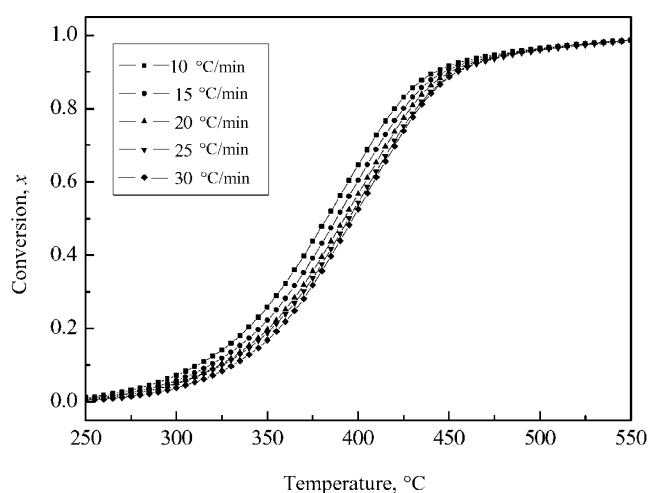


Fig. 2. The  $x-t$  curves of oil shale at different heating rates. The data of temperature  $T$  versus reaction rate  $dx/dt$  can be determined by Eq. (1), as shown in Fig. 3.

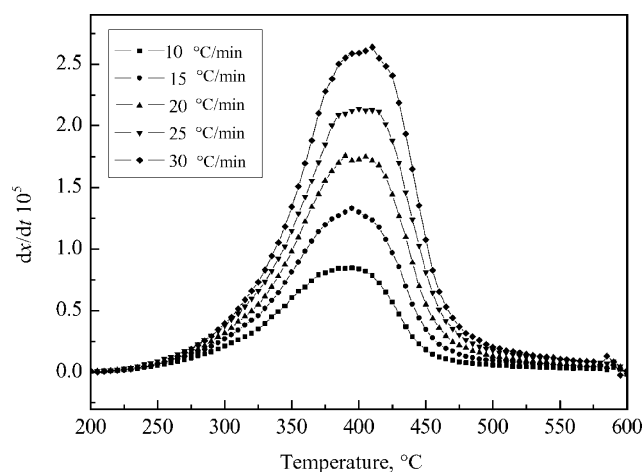


Fig. 3. The  $dx/dt$  curves of oil shale at different heating rates.

Furthermore, the higher the heating rate, the lower the conversion at a steady temperature. For example, when the temperature reaches 400 °C at five different constant heating rates of 10, 15, 20, 25 and 30 °C/min, the conversions are 0.92, 0.91, 0.90, 0.89 and 0.89, respectively. It is because the rates of heat transfer at various heating rates are different, and the shorter the exposure time at a particular temperature, the higher the heating rate, as well as the effect of decomposition kinetics [14, 15].

### Results from Friedman procedure

According to Eq. (5), 19 values of fractional conversion  $x$  were selected, ranging from 0.05 to 0.95, at equal intervals of 0.05. The values of  $dx/dt$  and  $T$  were determined for each  $x$  value of different heating rates. From the slope and intercept of  $\ln dx/dt$  vs.  $1/T$ , different values of  $E$  and  $A$  were calculated for each  $x$ . The results are shown in Table 1.

Table 1. Results calculated using Friedman procedure

$x$	$E$ , kJ/mol	$A$ , sec <sup>-1</sup>	Correlation coefficient
0.05	165.41	$1.13 \times 10^{10}$	0.998
0.10	184.39	$1.45 \times 10^{13}$	0.996
0.20	224.20	$1.62 \times 10^{16}$	0.996
0.30	253.71	$1.66 \times 10^{18}$	0.998
0.40	272.36	$2.16 \times 10^{19}$	0.997
0.50	282.63	$6.03 \times 10^{19}$	0.996
0.60	297.41	$7.45 \times 10^{20}$	0.997
0.70	308.46	$2.69 \times 10^{21}$	0.997
0.80	325.71	$1.79 \times 10^{22}$	0.998
0.90	374.07	$1.09 \times 10^{25}$	0.997
0.95	544.59	$1.80 \times 10^{35}$	0.996

As shown in Table 1, when conversion ranges from 0.05 to 0.95, the values of activation energies are in the range of 165–545 kJ/mol, and the correlation coefficients exceed 0.99. Moreover, as conversion degree increases, the activation energies increase as well. Because the oil shale kerogen is a kind of polymer with a three-dimensional structure, its pyrolysis process may involve the rupture of different types of chemical bonds with different activation energies. During the heating process, reactions with low activation energies proceed firstly to produce shale oil and gas, such as the rupture of C–O, C–S, and the branched function groups in kerogen. With increasing temperature, bonds with higher energies will gradually be ruptured needing higher activation energies, such as the rupture of side chains in  $\beta$ -site aromatics, decomposition of normal alkenes of large molecular mass, Diels-Alder cyclation reaction and the decomposition of alicyclic hydrocarbons [16, 17].

From Table 1 it is also seen that there is a good linear relationship between the logarithm of frequency factor and activation energies. The results of linear fitting are shown in Fig. 4, the regression equation is  $\ln A = 0.1498E - 0.3901$ , and linear correlation coefficient is 0.998. The regression equation of  $\ln A-E$  shows that exponential functions can be used to express the relationships between activation energy and frequency factor during oil shale pyrolysis. These relationships are important for us to understand the pyrolysis mechanism and to investigate the chemical structure of oil shale kerogen.

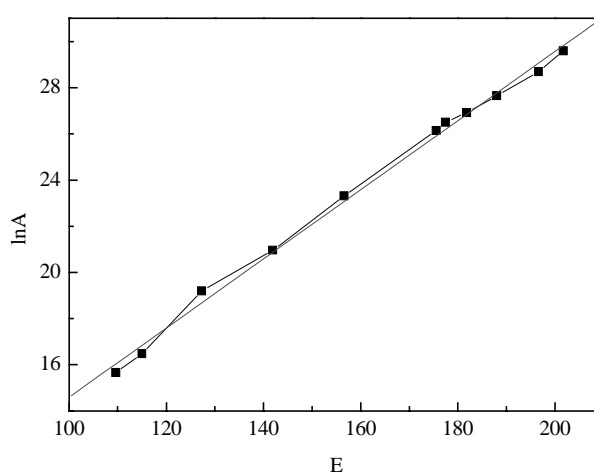


Fig. 4.  $\ln A-E$  relationships curves.

### Results from global first-order kinetics and pyrolysis time

Although the global first-order equation simply describes the process of oil shale pyrolysis, it enables readily to calculate the values of activation energy and frequency factor, and the result is unambiguous. The experimental data measured at different heating rates are respectively regressed linearly by Eq. (8), and the reaction kinetic parameters are presented in Table 2.

Table 2. Results from global first-order case

Heating rate, °C/min	$E$ , kJ/mol	$A$ , $\text{sec}^{-1}$	Correlation coefficient
10	168.92	$2.47 \times 10^{10}$	0.996
15	174.32	$5.18 \times 10^{10}$	0.993
20	180.39	$1.06 \times 10^{11}$	0.995
25	183.04	$1.49 \times 10^{11}$	0.994
30	187.79	$2.63 \times 10^{11}$	0.991

It is seen from Table 2 that the relative correlation coefficients of the first-order equation are close to unity and activation energies, calculated for different heating rates, are in a good linear relationship with heating rate. The relationship between logarithm of frequency factor and activation energy is linear as well. The results of linear fitting are shown in Fig. 5 and Fig. 6 and the regression equations are:

$$E = 0.9293\beta + 160.31 \quad (R=0.986), \quad (10)$$

$$\ln A = 0.1246E + 2.9083 \quad (R=0.999). \quad (11)$$

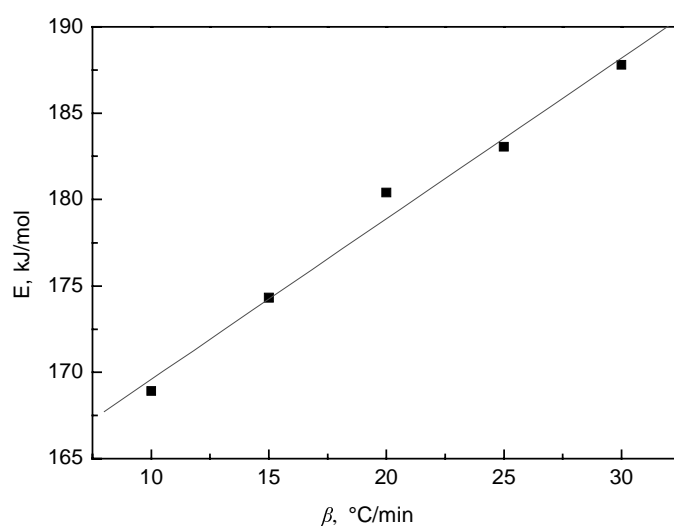


Fig. 5.  $\beta$ - $E$  relationships curves.

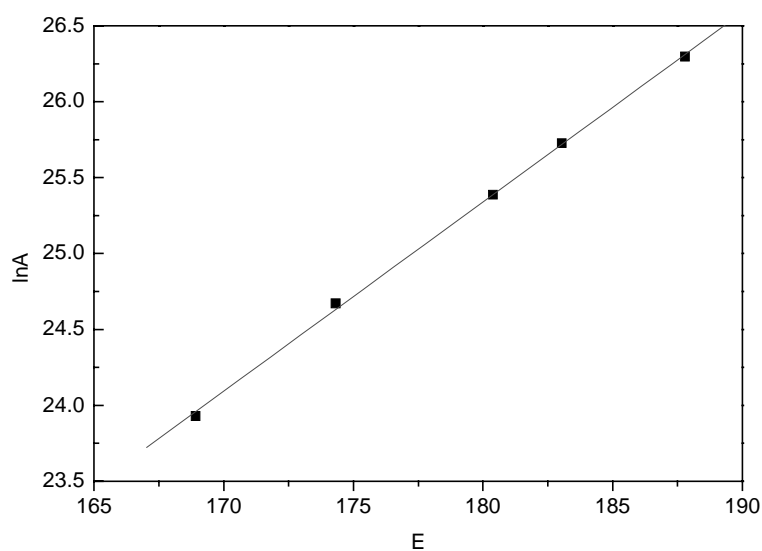


Fig. 6.  $\ln A$ - $E$  relationships curves.

According to the regression equation, when the heating rate decreases to zero (it means isothermal pyrolysis), the value of activation energy will be 160.31 kJ/mol and the frequency factor  $8.67 \times 10^9 \text{ s}^{-1}$ . When conversion is 0.95 and heating rate is zero, substituting the frequency factor and activation energy into Eq. (9) yields

$$t = 3.46 \times 10^{-10} e^{\frac{1.928 \times 10^4}{T}} . \quad (12)$$

From Eq. (12), the pyrolysis times are predicted at each constant temperature from 375 °C to 550 °C as shown in Fig. 7. It enables to predict the duration of oil shale pyrolysis at retorting. Eq. (12) shows that there is an exponential attenuation relationship between pyrolysis time and temperature, which refers to as time and temperature compensation in geochemistry fields. In other words, when the chemical and physical properties of oil shales are similar, the higher the temperature, the shorter the pyrolysis time.

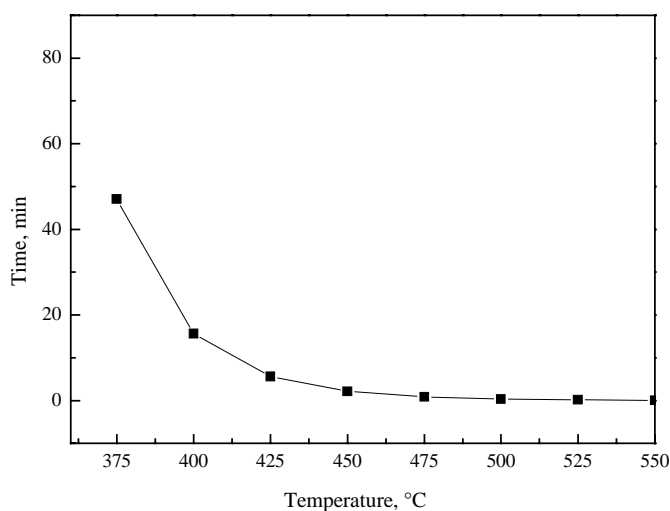


Fig. 7. Pyrolysis duration at various temperatures, needed to reach 95% conversion.

## Conclusions

The following conclusions can be drawn:

1. The changes in the trend curve of conversion *vs.* temperature are roughly the same at different heating rates. Furthermore, as the heating rate decreases, the conversion at a steady temperature will increase as well.
2. The apparent activation energies calculated for oil shale pyrolysis were in the range of 165-545 kJ/mol by Friedman procedure. In

addition, the  $\ln A$  and  $E$  are in a good linear relationship  $\ln A = 0.1498E - 0.3901$ .

3. Knowing the values of frequency factor and activation energy, calculated using the global first-order kinetic equation at different heating rates, pyrolysis time can be calculated –  $t = 3.46 \times 10^{-10} e^{\frac{1.928 \times 10^4}{T}}$ . The equation reveals that the higher the temperature, the shorter the pyrolysis time.

### Acknowledgements

This work is funded by Chinese national key science and technology special project (Grant No.. 2008ZX05018).

### REFERENCES

1. *Qian Jia-lin, Li Shu-yuan, Wang Jian-qiu*. World oil shale development & Utilization Trends. Report on 27<sup>th</sup> International Oil Shale Conference in Colorado, America, Sino-Global Energy (Chinese). 2008. Vol. 13, No. 1. P. 11–15 [in Chinese].
2. *Carroll, A*. Upper Permian Oil Shale Deposits of Northwest China: World's Largest? 27<sup>th</sup> Oil Shale Symposium, Paper No. 13.4, Colorado School of Mines, Golden, Colorado, 2007.
3. *Hu Wen-rui*. Development and potential of unconventional oil and gas resources in China National Petroleum Corporation // Natural Gas Industry. 2008. Vol. 28, No. 7. P. 5–7 [in Chinese].
4. *Yen, T. F*. Structure investigate on Green River oil shale // Science and Technology of Oil Shale / Yen, T. F. (ed.). – Ann Arbor, MI: Ann Arbor Science Publishers, 1976.
5. *Hartman-Stroup, C*. The effect of organic matter type and organic carbon content on Rock-Eval hydrogen index in oil shales and source rocks // Org. Geochem. 1987. Vol. 11, No. 5. P. 351–369.
6. *Sykes, R., Snowdon, L. R*. Guidelines for assessing the petroleum potential of coaly source rocks using Rock-Eval pyrolysis // Org. Geochem. 2002. Vol. 33, No. 12. P. 1441–1455.
7. *Spiro, B*. Effects of minerals on Rock Eval pyrolysis of kerogen // J. Therm. Anal. Calorim. 1991. Vol. 37, No. 7. P. 1513–1522.
8. *Rahman, M., Herod, A. A., Kandiyoti, R*. Correlation of the Rock-Eval hydrocarbon index with yields of pyrolysis oils and volatiles determined in a wire-mesh reactor // Fuel. 2000. Vol. 79, No. 2. P. 201–205.
9. *Baskin, D. K*. Atomic H/C ratio of kerogen as an estimate of thermal maturity and organic matter conversion // AAPG Bulletin. 1997. Vol. 81, No. 9. P. 1437–1450.
10. *Boudou, J.-P*. Relations between Rock-Eval  $T_{\max}$  and other parameters in a sedimentologically homogeneous coal series // Fuel. 1984. Vol. 63, No. 3. P. 430–431.

11. *Johannes, I., Kruusement, K., Palu, V., Veski, R., Bojesen-Koefoed, J. A.* Evaluation of oil potential of Estonian oil shales and biomass samples using Rock-Eval analyzer // *Oil Shale*. 2006. Vol. 23, No. 2. P. 110–118.
12. *Lewan, M. D., Hill, R. J., Ruble, T. E.* Comparison of oil generation kinetics for oil shales as determined by Rock-Eval and hydrous pyrolysis. 27<sup>th</sup> Oil Shale Symposium, Paper No. 10.2, Colorado School of Mines, Golden, Colorado, 2007.
13. *Wen Shi-peng.* Applied Numerical Analysis. – Beijing: Petroleum Industry Press, 1999 [in Chinese].
14. *Nazzal, J. M.* Influence of heating rate on the pyrolysis of Jordan oil shale // *J. Anal. Appl. Pyrol.* 2002. Vol. 62, No. 2. P. 225–238.
15. *Rajeshwar, K.* Thermal analysis of coal, oil shale and oil sand // *Thermochim. Acta*. 1983. Vol. 63, No. 1. P. 97–112.
16. *Li Shuyuan, Yue Changtao.* Study of different kinetic models for oil shale pyrolysis // *Fuel Process. Technol.* 2003. Vol. 85, No. 1. P. 51–61.
17. *Li Shuyuan, Yue Changtao* // *Fuel*. 2003. Vol. 82, No. 3. P. 337–342.

*Presented by V. Oja*

Received July 20, 2009